Lithology and fluid differentiation using rock physics template

Xin-gang Chi and De-hua Han, University of Houston

The elastic properties such as velocity, density, impedance, and V_P/V_S ratio take an important role in reservoir characterization because they are related to the reservoir properties. To analyze these elastic properties, rock physics knowledge is a bridge that links the elastic properties to the reservoir properties such as water saturation, porosity, and shale volume. In this study, we build up a rock physics template and plot it along with the inverted elastic properties to aid the efficient interpretation. Using this method, we can estimate the lithology and fluid content of undrilled areas if the undrilled area has the same geological deposition environment as a drilled area. The final results show that the lithology and fluid content can be efficiently interpreted for our target reservoirs using the inverted elastic properties plotted with a rock physics template, rather than only using the inverted elastic properties.

Rock physics is an indispensable tool for an efficient interpretation, providing the basic relationship between the lithology, fluid, and geological deposition environment of the reservoir. Also, rock physics modeling can be utilized to build a template for efficient reservoir characterization (Ødegaard and Avseth, 2004; Avseth et al., 2006; Andersen and Wijngaarden, 2007). In reservoir property analysis, the lithology and fluid content or saturation cannot be predicted efficiently by identifying different clusters in the cross-plot of elastic properties. In contrast, the elastic properties inverted from seismic data can be efficiently interpreted in conjunction with a rock physics template, which in turn can be used to predict lithology and fluid content.

We apply the rock physics template posted with the inverted velocities and density together to aid the interpretation to differentiate the reservoir lithology and fluid content in this study.

Rock physics template

To generate a rock physics template, we first use the Hertz-Mindlin contact theory (Mindlin, 1949) to construct the dry modulus of the rock at the high-porosity end number, which is pressure-dependent. Then, we construct the other end point as the modulus of the dry rock at zero porosity to be the modulus of the solid mineral. Between the high-porosity and zero-porosity end members, the modulus of the dry rock can be estimated based the Hashin-Shtrikman (1963) bounds, which give the theoretical predictions of the effective elastic modulus of a mixture of grains and pores. For an unconsolidated sand reservoir, the lower Hashin-Shtrikman bound is applied. For a cemented reservoir, the upper Hashin-Shtrikman bound should be utilized.

The Hashin-Shtrikman bounds are the bounds that show the narrowest possible modulus range without specifying anything about the pore geometries. The physical picture is that one material fills the pores and another material constructs the shell. The upper and lower bounds can be calculat-
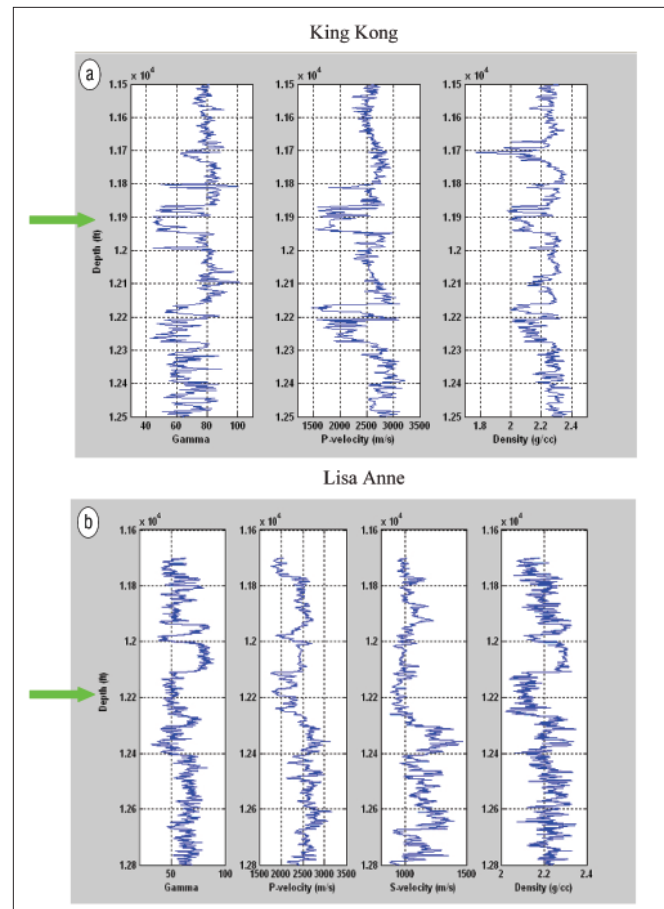

Figure 1. *The well logs of King Kong and Lisa Anne. At each area, the target reservoir is the unconsolidated sand with lower P-velocity and density than the top and bottom shale layers. The fluid in the target reservoir at each area is gas, water, or a mixture of both.*

ed simply by exchanging the two materials. When the stiffer material is distributed in the shell, the upper bound can be estimated. When it is in the core, the lower bound can be estimated. The Hashin-Shtrikman bounds can be applied to mixtures of more than two phases. The assumption of this model is that each component and the rock are isotropic and elastic (Mavko et al., 1998).

Gassmann's equation is applied to estimate the fluid substitution effect in a rock physics template and thereby the elastic modulus of dry and saturated rock. The pore fluid properties are controlled by reservoir pressure, temperature, and water saturation. In the forward modeling, we assume the fluid is uniformly rather than patchily distributed in the rock. The reservoir fluid in this study is gas, water, or a mixture of both.

Application

The method is applied in the seismic datasets, which are acquired from two areas in the deepwater Gulf of Mexico: King Kong and Lisa Anne (O'Brien, 2004). The targets in
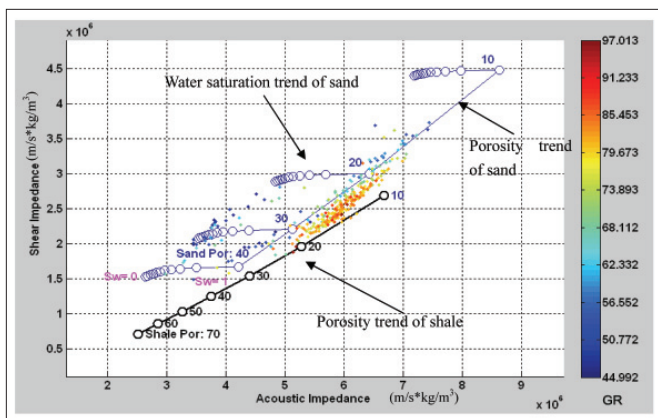
Figure 2. *The rock physics template posted in the cross plot of acoustic impedance versus shear impedance calculated from well log data at King Kong. The points with low acoustic impedance show the high porosity and gas saturation. The points between the porosity trend of sand and the porosity trend of shale show the shaly sand and sandy shale.*
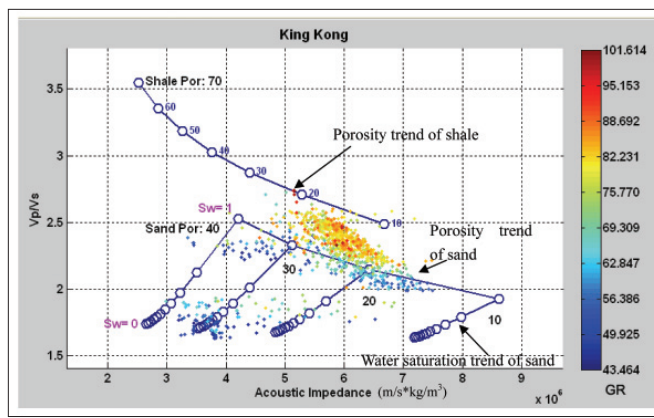

Figure 4. *The rock physics template posted in the cross plot of acoustic impedance versus V_P/V_S ratio calculated from well log data at King Kong. The points with low acoustic impedance and V_P/V_S ratio show the high porosity and high gas saturation.*
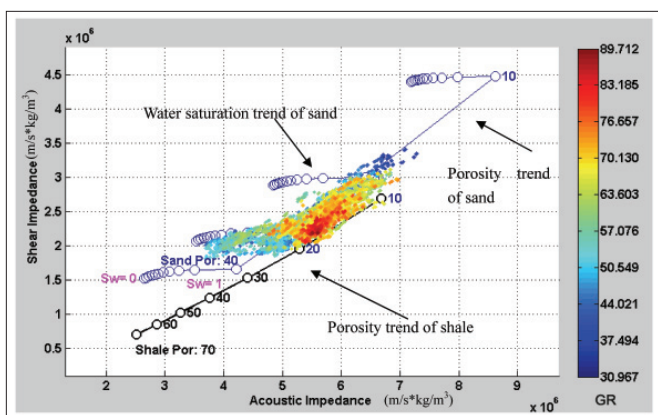

Figure 3. *The rock physics template posted in the cross-plot of acoustic impedance versus shear impedance calculated from well log data at Lisa Anne. The points with low acoustic impedance show the low gas saturation and high porosity.*
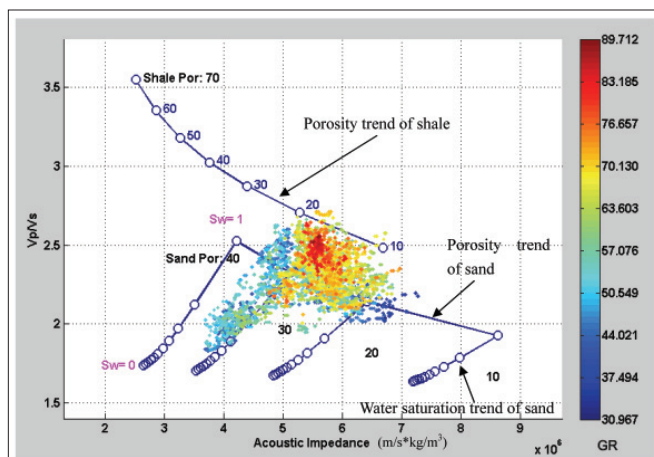

Figure 5. *The rock physics template posted in the cross-plot of acoustic impedance versus V_P/V_S ratio calculated from well log data at Lisa Anne. The points with low acoustic impedance show the low gas saturation and high porosity.*

both fields are unconsolidated sand reservoirs

Figure 1(a) shows the King Kong well logs. At a depth of about 11 900 ft (green arrow), there is a sand reservoir zone with low velocity, low gamma ray, and low density. We estimate the shear velocity using the Greenberg and Castagna method (1992). This reservoir is an unconsolidated sand reservoir with high porosity and low shale volume. The lowest P-velocity is approximately 1600 m/s, and the density is approximately 2.0g/cc for the gas-saturated sand in this area. Figure 1(b) shows the Lisa Anne well logs are plotted against the depth. At a depth of about 12 200 ft, there is one sand zone (green arrow) with low gamma ray, low velocity, and low density. The P-velocity of this reservoir is about 1700 m/s, and the density of this reservoir is lower than 2.1 g/cc.

From Lisa Anne well logs, the elastic properties such as P-velocity, S-velocity, and density are read for sand and shale, respectively. The input parameters of the forward rock physics model are derived by matching the elastic properties generated from the forward rock physics modeling with the elastic properties read from the well logs. Therefore, the rock physics template can be generated using the forward rock physics

model and the well logs of Lisa Anne. Then, the rock physics template is posted on the cross-plots of acoustic impedance versus shear impedance, which are calculated from well logs of King Kong and Lisa Anne (Figure 2 and Figure 3). Also, the same rock physics template is posted on the cross-plots of V_P/V_S ratio versus acoustic impedance calculated from well logs of King Kong and Lisa Anne (Figure 4 and Figure 5). Even though the rock physics template is only calibrated using Lisa Anne well logs, it is applicable at King Kong since these two areas have very similar geological deposition environment. Thus, we can predict the lithology and fluid content at undrilled areas using Lisa Anne well logs as a reference if we assume those areas have the similar geological deposition environment to Lisa Anne.

In this study, we simultaneously invert the P-velocity, S-velocity, and density using the prestack seismic angle gathers. To predict and analyze the lithology and fluid content along the horizons of King Kong and Lisa Anne reservoir tops, we derive the acoustic impedance, shear impedance, and V_P/V_S ratio in Figure 6 using the inverted velocities and density. With the posted rock physics template in the cross plots of
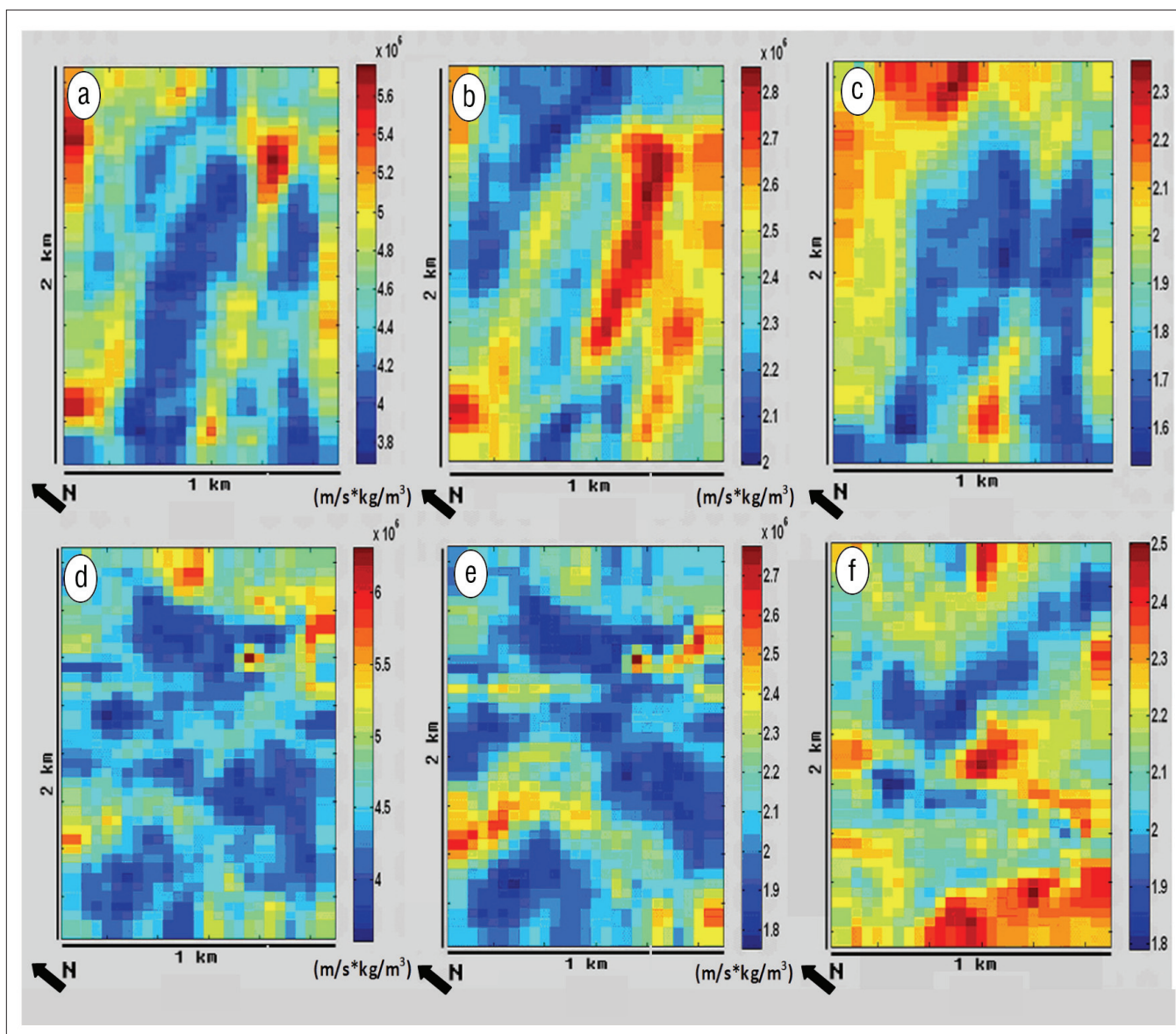
Figure 6. *The derived impedances and V_P/V_S ratios along the reservoir tops. (a) The acoustic impedance at King Kong. (b) The shear impedance at King Kong. (c) The V_P/V_S ratio at King Kong. (d) The acoustic impedance at Lisa Anne. (e) The shear impedance at Lisa Anne. (f) The V_P/V_S ratio at Lisa Anne. The wells are drilled in the center of these map views for King Kong and Lisa Anne.*

the inverted elastic properties, we are able to analyze and interpret the final inversion results.

Examining the cross plots in Figure 7, it is difficult to differentiate the gas-saturated zone without the rock physics template for King Kong and Lisa Anne. Thus, the rock physics template needs to be viewed along with the inverted elastic properties in the cross plots to reduce risk for the interpretation. The inverted elastic properties are plotted with the rock physics templates in Figure 8 and Figure 9. Whether in the cross plots of acoustic impedance versus shear impedance or in the cross plots of acoustic impedance versus V_P/V_S ratio, the inverted elastic properties of King Kong show distribution of the gas-saturated zone, and the inverted elastic properties of Lisa Anne do not. The gas-saturated zone of King Kong is selected in the left and lower side indicated by the green box in Figure 10. Figure 10 also shows the picked seismic amplitude

along the reservoir top of King Kong; the commercial gas-saturated zone is plotted in blue based on the selected zone in Figure 10. The water-saturated zone is plotted in brown along the reservoir top of King Kong. Through these cross plots and the posted rock physics template, the reservoir lithology and fluid content can be interpreted clearly and efficiently for King Kong and Lisa Anne.

Conclusions

Using the cross-plots of elastic properties with the rock physics template, we can clearly delineate the lithology and fluid content. The prior information such as well log, core, and geological modeling can help construct the rock physics template and includes the effects of pressure, temperature, and fluid property. The lithology and fluid content of undrilled areas can be predicted using the drilled well information as
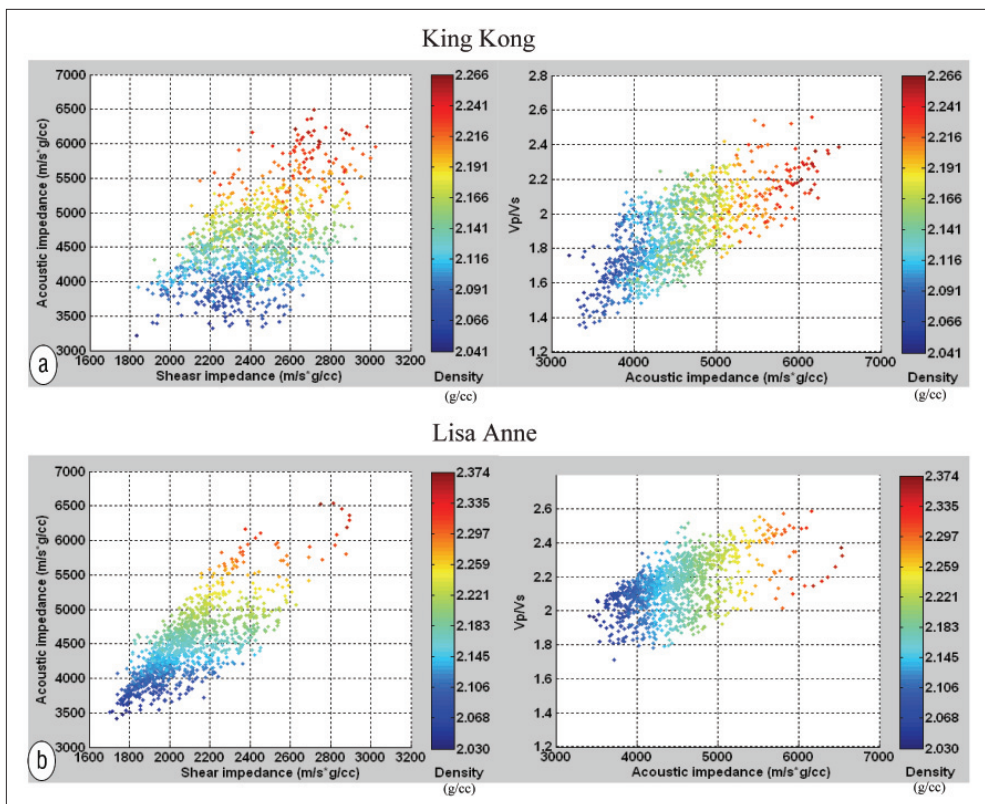
Figure 7. The cross plots of the elastic properties inverted from seismic data at King Kong and Lisa Anne. The points with low-acoustic impedance are corresponding to the sand reservoir. The reservoir fluid is not easily differentiated for King Kong and Lisa Anne only base on these cross plots.
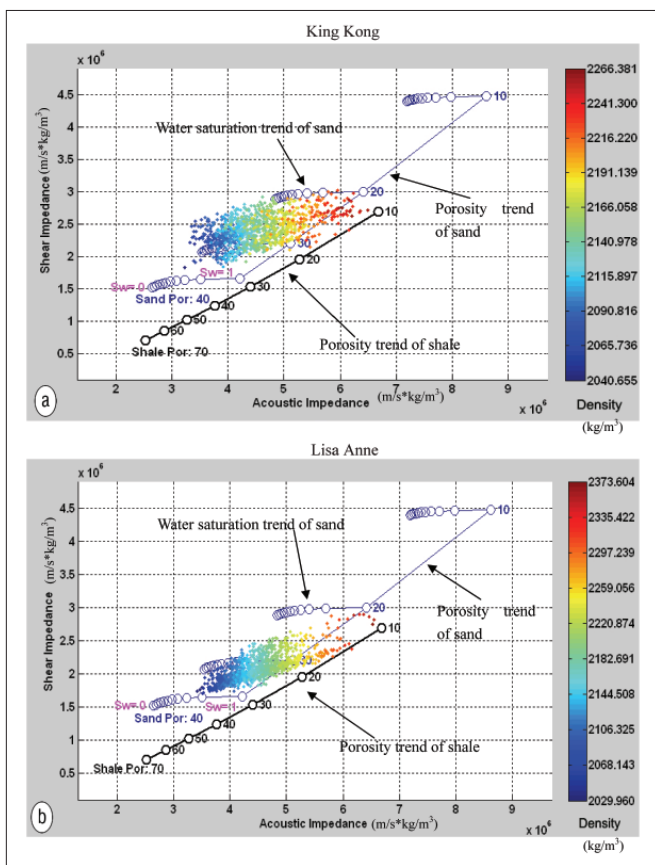

Figure 8. The rock physics template posted in the cross-plot of the acoustic impedance versus shear impedance inverted from seismic data at King Kong and Lisa Anne. Comparing (a) and (b), King Kong reservoir has a little lower porosity than Lisa Anne reservoir. King Kong reservoir is gas-saturated and Lisa Anne reservoir is water-saturated.
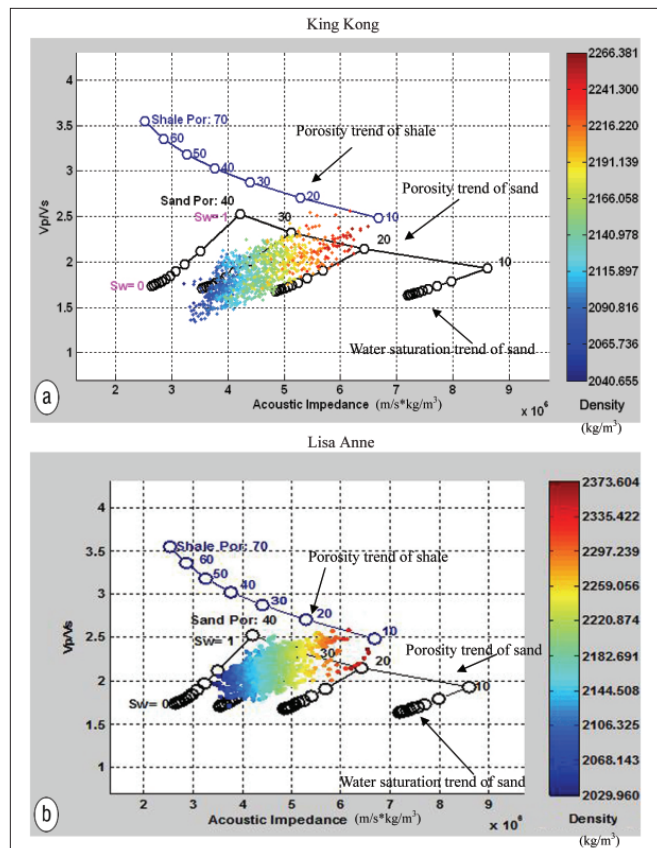

Figure 9. The rock physics template posted in the cross plot of acoustic impedance versus V_P/V_S ratio inverted from seismic data at King Kong and Lisa Anne. Comparing (a) and (b), King Kong reservoir has higher gas saturation and lower porosity than the Lisa Anne reservoir, which is consistent with Figure 8.
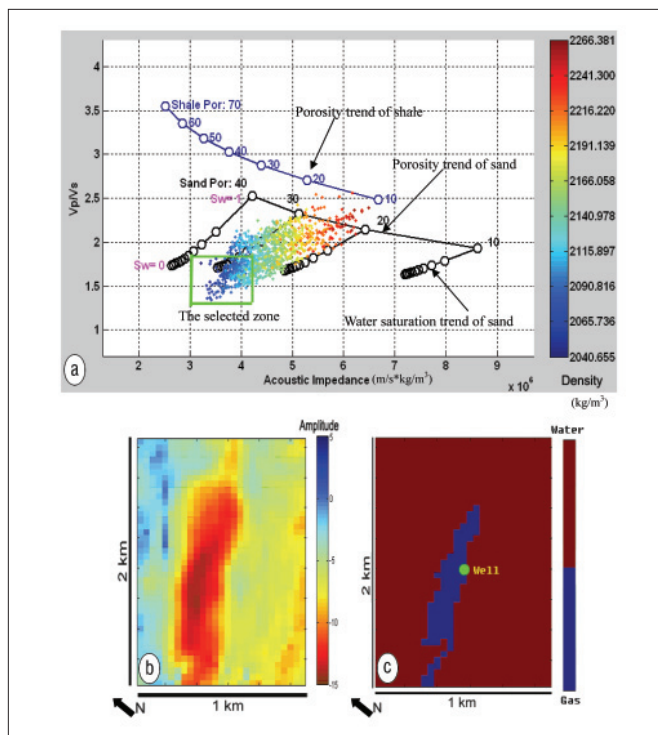
Figure 10. (a) The rock physics template posted in the cross-plot of acoustic impedance versus V_p/V_s ratio inverted from seismic data at King Kong with the selected zone (green box). (b) The picked seismic amplitude along the reservoir top. (c) The interpreted commercial gas-saturated zone along the reservoir top at King Kong is corresponding to the selected zone in (a). The green point in the center is the well location.

a reference if the undrilled areas have a similar geological deposition environment to the drilled area.

In this study, the well log data of Lisa Anne are utilized to calibrate the rock physics template for each area. Cross plotting elastic properties in conjunction with the rock physics templates demonstrates that King Kong reservoir is gas-saturated and Lisa Anne reservoir is fizz-saturated.

Suggested reading. "Interpretation of 4D AVO inversion results using rock physics templates and virtual reality visualization, North Sea examples" by Andersen and Wijngaarden (SEG 2007 *Expanded Abstracts*). "Combined porosity, saturation, and net-to-gross estimation from rock physics templates" by Avseth et al. (SEG 2006 *Expanded Abstracts*). "Shear-wave velocity estimation in porous rocks: Theoretical formulation, preliminary verification and applications," by Greenberg and Castagna (*Geophysical Prospecting*, 1992). "A variational approach to the elastic behavior of multiphase material" by Hashin and Shtrikman (*Journal of Mechanical Physical Solids*, 1963). *The Rock Physics Handbook* by Mavko et al. (Cambridge University Press, 1998). "Compliance of elastic bodies in contact" by Mindlin (*Journal of Applied Mechanics*, 1949). "Seismic amplitudes from low gas saturation sands" by O'Brien (*TLE*, 2004). "Well log and seismic data analysis using rock physics templates" by Ødegaard and Avseth (*First Break*, 2004). **TLE**